JOHANNES KEPLER UNIVERSITY LINZ

Institute of Computational Mathematics

IETI-DP Methods for Discontinuous Galerkin Multi-Patch Isogeometric Analysis with T-junctions

Rainer Schneckenleitner
Institute of Computational Mathematics, Johannes Kepler University
Altenberger Str. 69, 4040 Linz, Austria

Stefan Takacs
Johann Radon Institute for Computational and Applied Mathematics
Austrian Academy of Sciences
Altenberger Str. 69, 4040 Linz, Austria

NuMa-Report No. 2021-07 September 2021

Technical Reports before 1998:

1995

95-1	Hedwig Brandstetter *Was ist neu in Fortran 90?*	March 1995
95-2	G. Haase, B. Heise, M. Kuhn, U. Langer *Adaptive Domain Decomposition Methods for Finite and Boundary Element Equations.*	August 1995
95-3	Joachim Schöberl *An Automatic Mesh Generator Using Geometric Rules for Two and Three Space Dimensions.*	August 1995

1996

96-1	Ferdinand Kickinger *Automatic Mesh Generation for 3D Objects.*	February 1996
96-2	Mario Goppold, Gundolf Haase, Bodo Heise und Michael Kuhn *Preprocessing in BE/FE Domain Decomposition Methods.*	February 1996
96-3	Bodo Heise *A Mixed Variational Formulation for 3D Magnetostatics and its Finite Element Discretisation.*	February 1996
96-4	Bodo Heise und Michael Jung *Robust Parallel Newton-Multilevel Methods.*	February 1996
96-5	Ferdinand Kickinger *Algebraic Multigrid for Discrete Elliptic Second Order Problems.*	February 1996
96-6	Bodo Heise *A Mixed Variational Formulation for 3D Magnetostatics and its Finite Element Discretisation.*	May 1996
96-7	Michael Kuhn *Benchmarking for Boundary Element Methods.*	June 1996

1997

97-1	Bodo Heise, Michael Kuhn and Ulrich Langer *A Mixed Variational Formulation for 3D Magnetostatics in the Space $H(rot) \cap H(div)$*	February 1997
97-2	Joachim Schöberl *Robust Multigrid Preconditioning for Parameter Dependent Problems I: The Stokes-type Case.*	June 1997
97-3	Ferdinand Kickinger, Sergei V. Nepomnyaschikh, Ralf Pfau, Joachim Schöberl *Numerical Estimates of Inequalities in $H^{\frac{1}{2}}$.*	August 1997
97-4	Joachim Schöberl *Programmbeschreibung NAOMI 2D und Algebraic Multigrid.*	September 1997

From 1998 to 2008 technical reports were published by SFB013. Please see
`http://www.sfb013.uni-linz.ac.at/index.php?id=reports`
From 2004 on reports were also published by RICAM. Please see
`http://www.ricam.oeaw.ac.at/publications/list/`
For a complete list of NuMa reports see
`http://www.numa.uni-linz.ac.at/Publications/List/`

IETI-DP methods for discontinuous Galerkin multi-patch Isogeometric Analysis with T-junctions

Rainer Schneckenleitner* and Stefan Takacs†

Abstract

We study Dual-Primal Isogeometric Tearing and Interconnecting (IETI-DP) solvers for non-conforming multi-patch discretizations of a generalized Poisson problem. We realize the coupling between the patches using a symmetric interior penalty discontinuous Galerkin (SIPG) approach. Previously, we have assumed that the interfaces between patches always consist of whole edges. In this paper, we drop this requirement and allow T-junctions. This extension is vital for the consideration of sliding interfaces, for example between the rotor and the stator of an electrical motor. One critical part for the handling of T-junctions in IETI-DP solvers is the choice of the primal degrees of freedom. We propose to add all basis functions that are non-zero at any of the vertices to the primal space. Since there are several such basis functions at any T-junction, we call this concept "fat vertices". For this choice, we show a condition number bound that coincides with the bound for the conforming case.

1 Introduction

Isogeometric Analysis (IgA), [17], is an approach to discretize partial differential equations (PDEs) that has been designed in order to overcome difficulties related to meshing of the computational domain. In IgA, the computational domain is parameterized by geometry functions, which are commonly represented in terms of B-splines or non-uniform rational B-splines (NURBS). Such a representation is also used in state-of-the-art computer aided-design (CAD) software. Usually, one considers multiple patches, each parameterized with its own geometry function (multi-patch IgA). We consider the case of non-overlapping patches.

*schneckenleitner@numa.uni-linz.ac.at, Institute of Computational Mathematics, Johannes Kepler University Linz, Austria

†stefan.takacs@ricam.oeaw.ac.at, Johann Radon Institute Institute for Computational and Applied Mathematics, Austrian Academy of Sciences, Linz, Austria

Conforming discretizations require that both the geometry functions and the grids agree on each interface between two patches. If this is not the case, discontinuous Galerkin (dG) methods, particularly the symmetric interior penalty discontinuous Galerkin (SIPG) approach [3], are an appropriate option. For its adaptation to IgA, see [13, 15, 16, 26] and others. In these publications, it is assumed that the interfaces between two patches consist (in the two-dimensional case) of whole edges, which excludes the case of T-junctions between patches. Now, we include the case of T-junctions, which allows greater flexibility for the geometry modeling. This is of vital interest for the simulation of objects with sliding interfaces, like the interface between the rotor and the stator of an electrical motor, which serves as computational domain in our model problem. The PDE in the model problem is the Poisson equation, which can be motivated as a model for the magnetostatic potential. In general, sliding interfaces lead to a non-matching decomposition of the computational domain into patches. In two dimensions, this means that T-junctions between patches occur for most rotational angles.

So far, several approaches have been considered to handle such types of problems, including the more classical locked-step methods, cf. [24], the moving band technique, cf. [7], the Lagrange multiplier method, cf. [20], interpolation approaches, cf. [23]. More recently, mortar techniques, cf. [4, 9], domain interface methods, cf. [5] or discontinuous Galerkin methods, cf. [2] have been considered. Also combinations of different approaches have been proposed, see, e.g., [18].

We focus on the SIPG approach, the contribution of this paper is a fast solver for the linear system obtained from the proposed discretization. A canonical choice for domains with many non-overlapping patches are domain decomposition (DD) solvers, like the Dual-Primal Finite Element Tearing and Interconnecting (FETI-DP) method, cf. [10, 11]. These solvers have been adapted to IgA in [19] and are sometimes referred to as Dual-Primal Isogeometric Tearing and Interconnecting (IETI-DP) solvers. Recently, the authors have developed an analysis that is also explicit in the spline degree, see [25].

The IETI-DP solvers have been extended to discontinuous Galerkin discretizations in [13, 14, 15, 26], however T-junctions have not been covered by the analysis so far. Most components of the IETI-DP framework can easily be extended to domains with T-junctions, see [27] for a numerical study. One of the critical questions is the choice of the primal degrees of freedom. We propose to add all basis functions that are non-zero at a vertex to the primal space. This yields a number of basis functions for each T-junction that grows linearly with the spline degree (fat vertices). If a vertex is the corner of the respective patch, there is only one single non-zero basis function. This means that our choice coincides with the standard choice of corner values. We introduce a scaled Dirichlet preconditioner for the Schur complement formulation of the IETI-DP system. We show that the condition number of the preconditioned system

is bounded by

$$Cp\left(1+\log p+\max_{k=1,\dots,K}\log\frac{H_k}{h_k}\right)^2,$$

where the constant $C>0$ is independent of the grid sizes h_k, the patch sizes H_k, the spline degree p, the smoothness of the splines within the patches $\Omega^{(k)}$, and coefficient jumps between the patches. C depends on the geometry functions, the maximum number of patches that meet on any vertex, the minimal interface length and the quasi-uniformity of the grids within each patch.

The remainder of the paper is structured as follows. We introduce the model problem in Section 2 and its SIPG discretization in Section 3. In Section 4, we propose the IETI-DP solver. Numerical examples are presented in the subsequent Section 5. The paper is concluded with some final remarks in Section 6. The proof of the condition number bound is given in an Appendix.

2 The model problem

In this section, we introduce the model problem which we consider in this paper. We use the same notation as in [26]. To keep the paper self-contained, we introduce the notation in the following.

First, we introduce the computational domain. $\Omega\subset\mathbb{R}^2$ is a simply connected and bounded open Lipschitz domain, which is composed of K non-overlapping, simply connected open patches $\Omega^{(k)}$, i.e.,

$$\overline{\Omega}=\bigcup_{k=1}^{K}\overline{\Omega^{(k)}}\quad\text{and}\quad\Omega^{(k)}\cap\Omega^{(\ell)}=\emptyset\quad\text{for all}\quad k\neq\ell,$$

where $\overline{T}$ denotes the closure of the set T. We assume that every patch $\Omega^{(k)}$ is parameterized by a geometry function

$$G_k:\widehat{\Omega}:=(0,1)^2\to\Omega^{(k)}:=G_k(\widehat{\Omega})\subset\mathbb{R}^2, \tag{1}$$

that has a continuous extension to the closure of $\widehat{\Omega}$. In IgA, the geometry functions G_k are commonly represented in terms of B-splines or NURBS. For the presented analysis, it is not necessary to restrict ourselves to these representations, as long as the Jacobian of G_k and its inverse are uniformly bounded.

We use the common notation for the Lebesgue and Sobolev spaces $L_2(\Omega)$ and $H^s(\Omega)$, $s\in\mathbb{R}$, respectively. Those function spaces are equipped with the standard norms $\|\cdot\|_{L_2(\Omega)}$ and $\|\cdot\|_{H^s(\Omega)}$ and seminorms $|\cdot|_{H^s(\Omega)}$. As usual, $H^1_0(\Omega)\subset H^1(\Omega)$ denotes the subspace of functions vanishing on $\partial\Omega$.

The boundary value problem of interest reads as follows. Find $u \in H_0^1(\Omega)$ such that

$$\int_\Omega \alpha \nabla u \cdot \nabla v \, \mathrm{d}x = \int_\Omega f v \, \mathrm{d}x \qquad \text{for all} \qquad v \in H_0^1(\Omega), \tag{2}$$

with a given source function $f \in H^{-1}(\Omega)$ and a uniformly positive and bounded diffusion coefficient α, which is constant on each patch, i.e., we have

$$\alpha(x) = \alpha_k \quad \text{for all} \quad x \in \Omega^{(k)}$$

with $\alpha_k > 0$ for all $k = 1, \dots, K$. Since, for simplicity, we represent the Dirichlet boundary conditions in a strong sense, we assume that the pre-images $\widehat{\Gamma}_D^{(k)} := G_k^{-1}(\partial\Omega \cap \partial\Omega^{(k)})$ of the Dirichlet boundary $\Gamma_D = \partial\Omega$ consist of whole edges of the parameter domain $\widehat{\Omega}$. An alternative, where this restriction would not be necessary, would be a fully floating IETI-DP discretization.

3 The discretization using IgA and SIPG

In this section, we first introduce the patch-local discretization spaces, then we discuss the overall discretization. For the local discretization spaces, we restrict ourselves for simplicity to B-splines. Let $p \in \mathbb{N} := \{1, 2, 3, \dots\}$ be the spline degree, where we assume for simplicity that the degree is uniform for all patches. For each patch $k \in \{1, \dots, K\}$ and each spatial dimension $\delta \in \{1, 2\}$, we introduce a p-open knot vector

$$\Xi^{(k,\delta)} = (\xi_1^{(k,\delta)}, \dots, \xi_{n^{(k,\delta)}+p+1}^{(k,\delta)})$$

with $\xi_1^{(k,\delta)} = \cdots = \xi_{p+1}^{(k,\delta)} = 0$ and $\xi_{n^{(k,\delta)}}^{(k,\delta)} = \cdots = \xi_{n^{(k,\delta)}+p+1}^{(k,\delta)} = 1$, where each inner knot might be repeated up to p times. Depending on the p-open knot vector, we introduce a B-spline basis $(B[p, \Xi^{(k,\delta)}, i])_{i=1}^{n^{(k,\delta)}}$ via the Cox-de Boor formula, cf. [6, Eq. (2.1) and (2.2)]. The collection $(B[p, \Xi^{(k,\delta)}, i])_{i=1}^{n^{(k,\delta)}}$ spans the univariate B-spline discretization space

$$S[p, \Xi^{(k,\delta)}] := \operatorname{span}\{B^{(k,\delta)}[p, \Xi, 1], \dots, B^{(k,\delta)}[p, \Xi, n^{(k,\delta)}]\}.$$

We use the standard tensor-product B-spline space $\widehat{V}^{(k)}$ over $\widehat{\Omega}$, which is obtained from the tensor-product space of the two univariate spline spaces. The corresponding physical space $V^{(k)}$ of $\widehat{V}^{(k)}$ is defined by the pull-back principle, i.e.,

$$\widehat{V}^{(k)} := \{v \in S[p, \Xi^{(k,1)}] \otimes S[p, \Xi^{(k,2)}] \ : \ v|_{\widehat{\Gamma}_D^{(k)}} = 0\} \quad \text{and} \quad V^{(k)} := \widehat{V}^{(k)} \circ G_k^{-1}, \tag{3}$$

where $v|_T$ denotes the restriction of v to T (trace operator). The grid size $\widehat{h}_k$ on the parameter domain and h_k on the physical domain are defined by

$$\widehat{h}_k := \max_{\delta=1,2} \max\{\xi_{i+1}^{(k,\delta)} - \xi_i^{(k,\delta)} \ : \ i = 1, \dots, n^{(k,\delta)} + p\} \quad \text{and} \quad h_k := \widehat{h}_k \operatorname{diam}(\Omega^{(k)}).$$

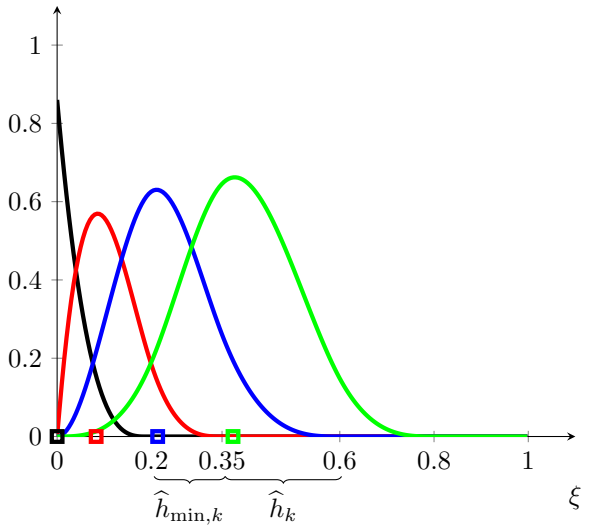

Figure 1: Basis functions in univariate case

Moreover, $\widehat{h}_{\min,k}$ denotes the smallest knot span, i.e., we define

$$\widehat{h}_{\min,k} := \min_{\delta=1,2} \min\{\xi_{i+1}^{(k,\delta)} - \xi_i^{(k,\delta)} \ : \ i = 1, \dots, n^{(k,\delta)} + p \text{ where } \xi_{i+1}^{(k,\delta)} \neq \xi_i^{(k,\delta)}\}.$$

Figure 1 shows the basis functions for the univariate case. Here and in what follows, we identify each basis function with its Greville point. We observe that there is only one active basis function on each end point of the interval; its Greville point is located on that end point.

Consequently, the standard tensor-product basis is represented as a grid of Greville points, cf. Figure 2, where an example with five patches is depicted. Note that, in the physical domain, the patches adjoin directly. Since we employ a discontinuous Galerkin discretization, the basis functions at the interfaces do not agree. Therefore, we separate the patches visually. The patches $\Omega^{(1)}$, $\Omega^{(3)}$, $\Omega^{(4)}$ and $\Omega^{(5)}$ meet in a regular corner. Certainly, it is also possible that only three or more than four patches meet in a regular corner. Such junctions have been previously considered. Here, we additionally allow T-junctions, like the junction between the patches $\Omega^{(1)}$, $\Omega^{(2)}$ and $\Omega^{(3)}$. Certainly, it is possible that more than three patches meet in a T-junction. Note that in any case, the T-junction constitutes a corner of every involved patch but one patch, like patch $\Omega^{(1)}$ in the example.

Having all patchwise discretization spaces defined, we obtain the global approximation space by

$$V := V^{(1)} \times \cdots \times V^{(K)}. \tag{4}$$

On this discontinuous discretization space, we introduce a variational formulation of the model problem (2) following the symmetric interior penalty discontinuous Galerkin (SIPG) method. Find $u = (u^{(1)}, \cdots, u^{(K)}) \in V$ such that

$$a_h(u, v) = \langle f, v \rangle \quad \text{for all} \quad v \in V, \tag{5}$$

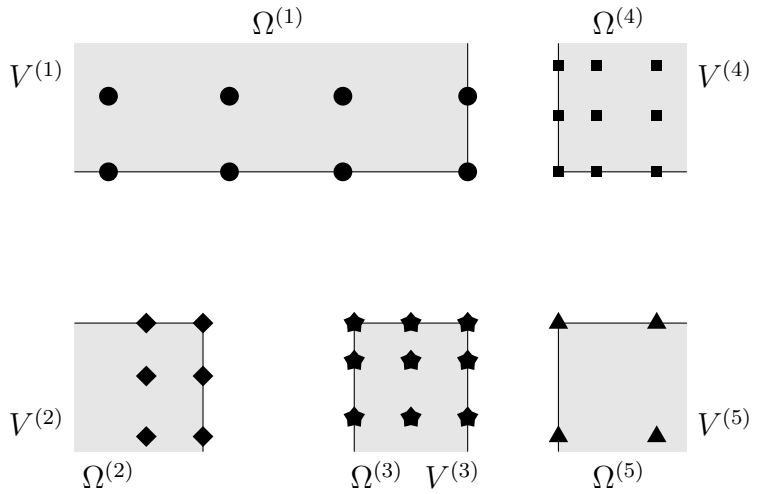

Figure 2: Schematic representation of local spaces

where

$$
\begin{aligned}
a_h(u,v) &:= \sum_{k=1}^{K} \left(a^{(k)}(u,v) + m^{(k)}(u,v) + r^{(k)}(u,v) \right), \\
a^{(k)}(u,v) &:= \int_{\Omega^{(k)}} \alpha_k \nabla u^{(k)} \cdot \nabla v^{(k)} \, \mathrm{d}x, \\
m^{(k)}(u,v) &:= \sum_{\ell \in \mathcal{N}_\Gamma(k)} \int_{\Gamma^{(k,\ell)}} \frac{\alpha_k}{2} \left(\frac{\partial u^{(k)}}{\partial n_k}(v^{(\ell)} - v^{(k)}) + \frac{\partial v^{(k)}}{\partial n_k}(u^{(\ell)} - u^{(k)}) \right) \mathrm{d}s, \\
r^{(k)}(u,v) &:= \sum_{\ell \in \mathcal{N}_\Gamma(k)} \int_{\Gamma^{(k,\ell)}} \alpha_k \frac{\delta p^2}{\min\{h_k, h_\ell\}} (u^{(\ell)} - u^{(k)})(v^{(\ell)} - v^{(k)}) \, \mathrm{d}s, \\
\langle f, v \rangle &:= \sum_{k=1}^{K} \int_{\Omega^{(k)}} f v^{(k)} \, \mathrm{d}x,
\end{aligned}
$$

and $\delta > 0$ is some suitably chosen penalty parameter and n_k is the unit normal vector pointing outwards of the patch $\Omega^{(k)}$ and $\Gamma^{(k,\ell)} := \partial\Omega^{(k)} \cap \partial\Omega^{(\ell)}$ is the interface between the two patches. $\mathcal{N}_\Gamma(k)$ contains the indices of the neighboring patches $\Omega^{(\ell)}$, sharing with $\Omega^{(k)}$ more than just a corner.

The penalty parameter δ ensures that the bilinear form $a_h(\cdot,\cdot)$ is bounded and coercive in the dG-norm

$$
\|v\|_d^2 := d(v,v), \qquad \text{where} \qquad d(u,v) := \sum_{k=1}^{K} \left(a^{(k)}(u,v) + r^{(k)}(u,v) \right).
$$

A suitable δ can always be chosen, independently of the spline degree p and grid sizes h_k, however it might depend on the geometry functions and on the quasi-uniformity of

the grids, i.e., the ratios $\widehat{h}_k/\widehat{h}_{\min,k}$, see [28, Theorem 8]. The Theorem of Lax-Milgram guarantees the existence and the uniqueness of a solution to (5). If the solution u of the continuous problem is sufficiently smooth, the solution of (5) is an approximation to the solution of the original problem (2), cf. [28, Theorems 12 and 13].

4 The dG IETI-DP solver

In this section, we introduce a IETI-DP solver for the discontinuous Galerkin discretization (5). The first step is the introduction of the local subspaces required for the domain decomposition method and the local assembling of the problem, see Subsection 4.1. In Subsection 4.2, we discuss the introduction of the primal degrees of freedom. Then, in Subsection 4.3, we discuss the coupling of the remaining degrees of freedom using Lagrange multipliers. The setup of the IETI system is discussed in Subsection 4.4, its solution is discussed in Subsection 4.5, and the corresponding convergence result is stated in Subsection 4.6.

4.1 Local subspaces and local problem

As it has been done in the seminal paper [19] and in follow-up publications on IETI-DP, the local spaces are constructed on a per-patch basis. For variational problems that are discretized using dG approaches, the setup of local spaces is not obvious. We follow the approach that has been first introduced in [8] and then adapted to IgA in [14, 13, 26, 27]: The introduction of artificial interfaces.

The local function space $V_e^{(k)}$ for a patch $\Omega^{(k)}$ is composed of the original function space $V^{(k)}$ of the patch and of the traces of the function spaces $V^{(\ell)}$, when restricted to the common interface $\Gamma^{(k,\ell)}$. Formally, we have

$$V_e^{(k)} := V^{(k)} \times \prod_{\ell \in \mathcal{N}_\Gamma(k)} V^{(k,\ell)}, \quad \text{where} \quad V^{(k,\ell)} := \{ v^{(\ell)}|_{\Gamma^{(k,\ell)}} \ : \ v^{(\ell)} \in V^{(\ell)} \}.$$

A local function $v_e^{(k)} \in V_e^{(k)}$ is represented as a tuple

$$v_e^{(k)} = \left(v^{(k)}, (v^{(k,\ell)})_{\ell \in \mathcal{N}_\Gamma(k)} \right), \quad \text{where} \quad v^{(k)} \in V^{(k)} \text{ and } v^{(k,\ell)} \in V^{(k,\ell)}. \tag{6}$$

The discretization space is visualized in Figure 3. Again, we depict the the interfaces and artificial interfaces separately since there live different function spaces. We again represent every basis function with its Greville point. Basis functions that origin from the same basis are denoted by the same symbol. The function spaces for the artificial interfaces, like $V^{(2,1)}$, are the traces of the corresponding spaces, here $V^{(1)}$. Their basis just consists of the traces of those basis functions of the basis of $V^{(1)}$ that are active on the interface $\Gamma^{(1,2)}$. While this is rather obvious for the case of interfaces that

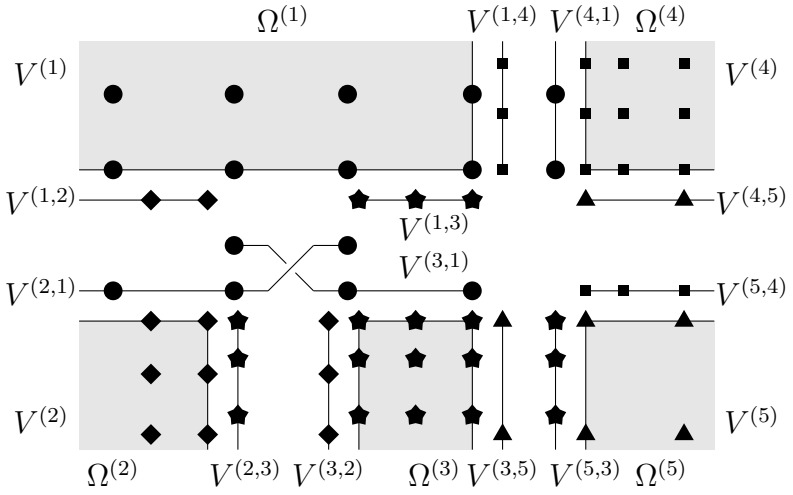

Figure 3: Schematic representation of local spaces with artificial interfaces

span over a whole edge, it needs some more elaboration in the context of T-junctions. As one can see in Figure 4, basis functions on the bottom side of the patch $\Omega^{(1)}$ are chosen to be part of the artificial interface if they do not vanish on $\Gamma^{(1,2)}$. This includes basis functions whose Greville point is not located on $\Gamma^{(1,2)}$. The corresponding basis functions form a part of both, the basis for $V^{(2,1)}$ and the basis for $V^{(3,1)}$. In Figure 3, we depict these degrees of freedom on extensions of the artificial interfaces.

For the IETI formulation, we collect the spaces that share the first index together, so for example $V_e^{(1)}$ is composed of $V^{(1)}$, $V^{(1,2)}$, $V^{(1,3)}$, and $V^{(1,4)}$.

We introduce local bilinear forms $a_e^{(k)}(\cdot,\cdot)$ and $d_e^{(k)}(\cdot,\cdot)$ and the local linear functional $\langle f_e^{(k)},\cdot\rangle$ that live on the spaces $V_e^{(k)}$. They can be seen as the local counterparts to $a_h(\cdot,\cdot)$, $d(\cdot,\cdot)$, and $\langle f,\cdot\rangle$ and we define them by

$$\begin{aligned} a_e^{(k)}(u_e^{(k)},v_e^{(k)}) &:= a^{(k)}(u_e^{(k)},v_e^{(k)}) + m^{(k)}(u_e^{(k)},v_e^{(k)}) + r^{(k)}(u_e^{(k)},v_e^{(k)}),\\ d_e^{(k)}(u_e^{(k)},v_e^{(k)}) &:= a^{(k)}(u_e^{(k)},v_e^{(k)}) + r^{(k)}(u_e^{(k)},v_e^{(k)}),\\ \langle f_e^{(k)},v_e^{(k)}\rangle &:= \int_{\Omega^{(k)}} f v^{(k)} \mathrm{d}x, \end{aligned}$$

where we write with a slight abuse of notation

$$\begin{aligned} a^{(k)}(u_e^{(k)},v_e^{(k)}) &:= \int_{\Omega^{(k)}} \alpha_k \nabla u^{(k)} \cdot \nabla v^{(k)} \,\mathrm{d}x,\\ m^{(k)}(u_e^{(k)},v_e^{(k)}) &:= \sum_{\ell\in\mathcal{N}_\Gamma(k)} \int_{\Gamma^{(k,\ell)}} \frac{\alpha_k}{2}\left(\frac{\partial u^{(k)}}{\partial n_k}(v^{(k,\ell)}-v^{(k)}) + \frac{\partial v^{(k)}}{\partial n_k}(u^{(k,\ell)}-u^{(k)})\right) \mathrm{d}s,\\ r^{(k)}(u_e^{(k)},v_e^{(k)}) &:= \sum_{\ell\in\mathcal{N}_\Gamma(k)} \int_{\Gamma^{(k,\ell)}} \alpha_k \frac{\delta p^2}{\min\{h_k,h_\ell\}}(u^{(k,\ell)}-u^{(k)})(v^{(k,\ell)}-v^{(k)}) \,\mathrm{d}s. \end{aligned}$$

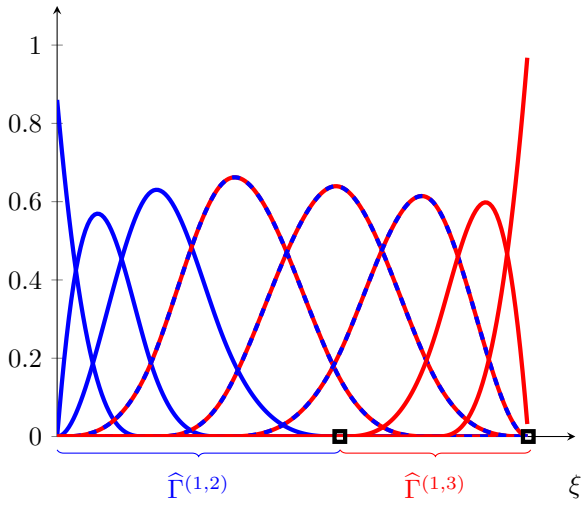

Figure 4: Basis functions selected for artificial interfaces; the dashed basis functions are selected for both bases

The discretization of $a_e^{(k)}(\cdot,\cdot)$ and $\langle f_e^{(k)},\cdot\rangle$ with respect to the chosen basis for $V_e^{(k)}$ gives the local linear system

$$A^{(k)}\,\underline{u}_e^{(k)} = \underline{f}_e^{(k)}. \tag{7}$$

4.2 Primal degrees of freedom

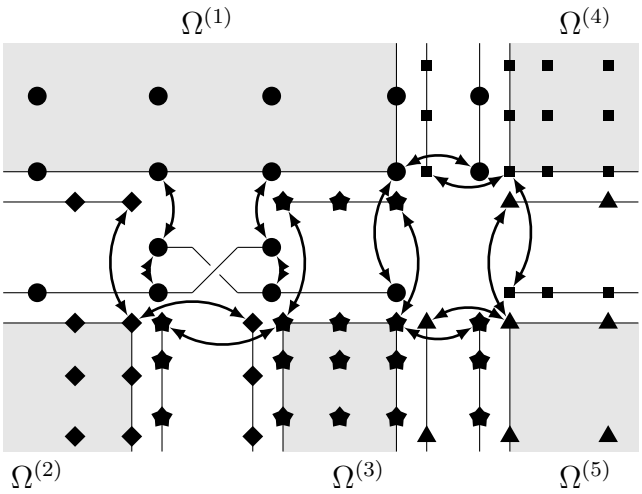

Figure 5: Primal constraints

Concerning the choice of the primal degrees of freedom, we follow the idea of vertex values. If a vertex $\mathbf{x}$ happens to be located on a corner of a patch $\Omega^{(k)}$, on each of the

corresponding patches, there is only one basis function active. In this case, the primal constraint enforces

$$u^{(k)}(\mathbf{x}) = u^{(\ell,k)}(\mathbf{x})$$

for all neighbors $\Omega^{(\ell)}$ that share the the vertex $\mathbf{x}$. The primal constraint is enforced by requiring that the coefficients for the corresponding basis function agree.

If a vertex happens to be a T-junction $\mathbf{x}$, we select all basis functions which do not vanish on the T-junction. All corresponding degrees of freedom are then treated as primal degrees of freedom. The primal constraint is again enforced by requiring that the coefficients for the corresponding basis functions agree.

The setup of the primal degrees of freedom is visualized in Figure 5.

4.3 Jump matrices and Lagrange multipliers

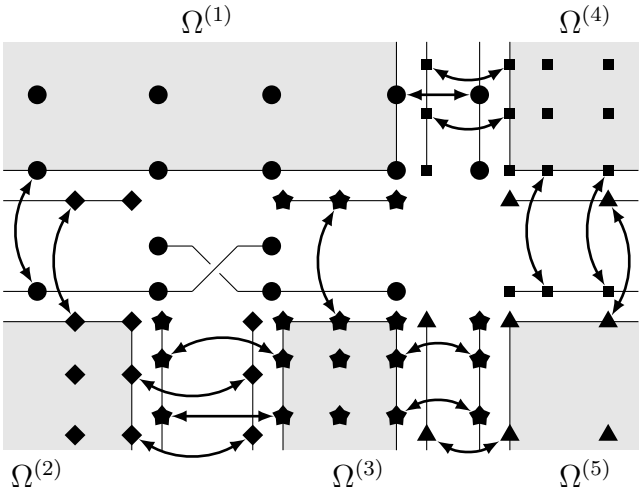

Figure 6: Action of the Lagrange multipliers

In the following, we introduce constraints that ensure the continuity of the solution between the interface on one patch and the corresponding artificial interfaces of the neighboring patches, i.e., between the function in $V^{(k)}$ and the functions in $V^{(\ell,k)}$. Note that the function spaces $V^{(k)}|_{\Gamma^{(k,\ell)}}$ and $V^{(\ell,k)}$ and the corresponding bases agree. This means that we obtain continuity if the corresponding coefficients agree. Since the primal degrees of freedom are enforced strongly, there are no constraints corresponding to the primal degrees of freedom, see Figure 6.

The constraints are represented by a matrix

$$B = \begin{pmatrix} B^{(1)} & \cdots & B^{(K)} \end{pmatrix},$$

where each row corresponds to one constraint enforcing the agreement of one of the coefficients in the usual way, i.e., such that every row has two non-zero entries: $+1$ and -1. The choice

$$B\underline{v} = 0,$$

corresponds to a function v that satisfies the constraints. Note that the proposed choice of primal degrees of freedom guarantees that there is no degree of freedom which is affected by more than one constraint. This is a property, which we use in the condition number analysis.

4.4 IETI system

Before we are able to setup the overall IETI system, we partition the degrees of freedom into the primal degrees of freedom (index Π), the degrees of freedom, which are subject to Lagrange multipliers, (index Δ), and the remaining, i.e., interior, degrees of freedom (index I). Using this partitioning, the matrices $A^{(k)}$, $B^{(k)}$ and the vector $\underline{f}_e^{(k)}$ have the following form:

$$A^{(k)} = \begin{pmatrix} A_{\mathrm{II}}^{(k)} & A_{\mathrm{I}\Delta}^{(k)} & A_{\mathrm{I}\Pi}^{(k)} \\ A_{\Delta\mathrm{I}}^{(k)} & A_{\Delta\Delta}^{(k)} & A_{\Delta\Pi}^{(k)} \\ A_{\Pi\mathrm{I}}^{(k)} & A_{\Pi\Delta}^{(k)} & A_{\Pi\Pi}^{(k)} \end{pmatrix}, \qquad B^{(k)} = \underbrace{\begin{pmatrix} B_{\mathrm{I}}^{(k)} & B_{\Delta}^{(k)} & B_{\Pi}^{(k)} \end{pmatrix}}_{= \begin{pmatrix} 0 & B_{\Delta}^{(k)} & 0 \end{pmatrix}}, \quad \text{and} \quad \underline{f}_e^{(k)} = \begin{pmatrix} \underline{f}_{\mathrm{I}}^{(k)} \\ \underline{f}_{\Delta}^{(k)} \\ \underline{f}_{\Pi}^{(k)} \end{pmatrix}.$$

Here, we make use of the fact that there are no Lagrange multipliers that are acting on the interior degrees of freedom (and thus $B_{\mathrm{I}}^{(k)} = 0$) or on the primal degrees of freedom (and thus $B_{\Pi}^{(k)} = 0$).

On each patch we eliminate the primal degrees of freedom. So, we define

$$\widetilde{A}^{(k)} := \begin{pmatrix} A_{\mathrm{II}}^{(k)} & A_{\mathrm{I}\Delta}^{(k)} \\ A_{\Delta\mathrm{I}}^{(k)} & A_{\Delta\Delta}^{(k)} \end{pmatrix}, \qquad \widetilde{B}^{(k)} := \underbrace{\begin{pmatrix} B_{\mathrm{I}}^{(k)} & B_{\Delta}^{(k)} \end{pmatrix}}_{= \begin{pmatrix} 0 & B_{\Delta}^{(k)} \end{pmatrix}}, \quad \text{and} \quad \underline{\widetilde{f}}^{(k)} := \begin{pmatrix} \underline{f}_{\mathrm{I}}^{(k)} \\ \underline{f}_{\Delta}^{(k)} \end{pmatrix}.$$

These local matrices are collected to global matrices $A = \mathrm{diag}(A^{(1)}, \dots, A^{(K)})$, $\widetilde{A} = \mathrm{diag}(\widetilde{A}^{(1)}, \dots, \widetilde{A}^{(K)})$ and $\widetilde{B} = (\widetilde{B}^{(1)}, \dots, \widetilde{B}^{(K)})$, and the local vectors into global vectors $\underline{\widetilde{f}} = ((\underline{\widetilde{f}}^{(1)})^\top, \dots, (\underline{\widetilde{f}}^{(K)})^\top)^\top$ and $\underline{f} = ((\underline{f}_e{}^{(1)})^\top, \dots, (\underline{f}_e{}^{(K)})^\top)^\top$.

For the setup of the primal problem, we introduce an A-orthogonal basis. To do so, we first introduce for each patch an $A^{(k)}$-orthogonal basis via

$$\Psi^{(k)} := \begin{pmatrix} A_{\mathrm{II}}^{(k)} & A_{\mathrm{I}\Delta}^{(k)} & 0 \\ A_{\Delta\mathrm{I}}^{(k)} & A_{\Delta\Delta}^{(k)} & 0 \\ 0 & 0 & I \end{pmatrix}^{-1} \begin{pmatrix} -A_{\mathrm{I}\Pi}^{(k)} \\ -A_{\Delta\Pi}^{(k)} \\ I \end{pmatrix}.$$

Let $R^{(k)}$ be a binary matrix that restricts a global coefficient vector of the primal degrees of freedom to the primal degrees that are associated to space $V_e^{(k)}$. Then, we

obtain the matrix representing the global A-orthogonal basis for the primal degrees of freedom via

$$\Psi := \begin{pmatrix} \Psi^{(1)} R^{(1)} \\ \vdots \\ \Psi^{(K)} R^{(K)} \end{pmatrix}.$$

The overall IETI-DP system reads as follows. Find $(\widetilde{\underline{u}}^\top, \underline{u}_\Pi^\top, \underline{\lambda}^\top)^\top$ such that

$$\begin{pmatrix} \widetilde{A} & & \widetilde{B}^\top \\ & \Psi^\top A \Psi & \Psi^\top B^\top \\ \widetilde{B} & B\Psi & \end{pmatrix} \begin{pmatrix} \widetilde{\underline{u}} \\ \underline{u}_\Pi \\ \underline{\lambda} \end{pmatrix} = \begin{pmatrix} \widetilde{\underline{f}} \\ \Psi^\top \underline{f} \\ 0 \end{pmatrix}. \tag{8}$$

This problem is equivalent to the original problem (5), cf. [21].

Remark 4.1. *In this paper, we follow the approach to eliminate the primal degrees of freedom, which is a commonly used approach for handling the corner values in actual implementations. Alternatively, one can incorporate the primal constraints using Lagrange multipliers, which is a common approach if edge averages are used as primal degrees of freedom. Certainly, this approach is also possible in the framework of this paper. Here, we would obtain the formulation* (8)*, however with the choice*

$$\widetilde{A}^{(k)} = \begin{pmatrix} A_{\Pi\Pi}^{(k)} & A_{\Pi\Delta}^{(k)} & A_{\Pi\Pi}^{(k)} & 0 \\ A_{\Delta\Pi}^{(k)} & A_{\Delta\Delta}^{(k)} & A_{\Delta\Pi}^{(k)} & 0 \\ A_{\Pi\Pi}^{(k)} & A_{\Pi\Delta}^{(k)} & A_{\Pi\Pi}^{(k)} & I \\ 0 & 0 & I & 0 \end{pmatrix}, \quad \widetilde{B}^{(k)} = \underbrace{\begin{pmatrix} B_\Pi^{(k)} & B_\Delta^{(k)} & B_\Pi^{(k)} & 0 \end{pmatrix}}_{= \begin{pmatrix} 0 & B_\Delta^{(k)} & 0 & 0 \end{pmatrix}}, \quad \widetilde{\underline{f}}_e^{(k)} = \begin{pmatrix} \underline{f}_\Pi^{(k)} \\ \underline{f}_\Delta^{(k)} \\ \underline{f}_\Pi^{(k)} \\ 0 \end{pmatrix}.$$

The matrix $(0\ 0\ I)$ *in the definition of* $\widetilde{A}^{(k)}$ *here is often called* $C^{(k)}$*.*

In theory papers, cf. [21], a FETI-DP or IETI-DP system is often written down in the equivalent skeleton formulation, which corresponds to the choice

$$\widetilde{A}^{(k)} = \begin{pmatrix} A_{\Delta\Delta}^{(k)} - A_{\Delta\Pi}^{(k)} (A_{\Pi\Pi}^{(k)})^{-1} A_{\Pi\Delta}^{(k)} & A_{\Delta\Pi}^{(k)} - A_{\Delta\Pi}^{(k)} (A_{\Pi\Pi}^{(k)})^{-1} A_{\Pi\Pi}^{(k)} & 0 \\ A_{\Pi\Delta}^{(k)} - A_{\Pi\Pi}^{(k)} (A_{\Pi\Pi}^{(k)})^{-1} A_{\Pi\Delta}^{(k)} & A_{\Pi\Pi}^{(k)} - A_{\Pi\Pi}^{(k)} (A_{\Pi\Pi}^{(k)})^{-1} A_{\Pi\Pi}^{(k)} & I \\ 0 & I & 0 \end{pmatrix},$$

$$\widetilde{B}^{(k)} = \begin{pmatrix} B_\Delta^{(k)} & B_\Pi^{(k)} & 0 \end{pmatrix} = \begin{pmatrix} B_\Delta^{(k)} & 0 & 0 \end{pmatrix}, \quad \textit{and} \quad \widetilde{\underline{f}}_e^{(k)} = \begin{pmatrix} \underline{f}_\Delta^{(k)} - A_{\Delta\Pi}^{(k)} (A_{\Pi\Pi}^{(k)})^{-1} \underline{f}_\Pi^{(k)} \\ \underline{f}_\Pi^{(k)} - A_{\Pi\Pi}^{(k)} (A_{\Pi\Pi}^{(k)})^{-1} \underline{f}_\Pi^{(k)} \\ 0 \end{pmatrix}.$$

4.5 Solving the IETI system

By applying a block-Gaussian elimination to (8), we obtain the Schur complement equation

$$F\, \underline{\lambda} = \underline{d}, \tag{9}$$

for the Lagrange multipliers $\underline{\lambda}$, where

$$F := \underbrace{\begin{pmatrix} \widetilde{B} & B\Psi \end{pmatrix} \begin{pmatrix} \widetilde{A} & \\ & \Psi^\top A \Psi \end{pmatrix}^{-1}}_{F_0 :=} \begin{pmatrix} \widetilde{B}^\top \\ \Psi^\top B^\top \end{pmatrix} \quad \text{and} \quad \underline{d} := F_0 \begin{pmatrix} \widetilde{f} \\ \Psi^\top \underline{f} \end{pmatrix}. \tag{10}$$

We solve (9) with a preconditioned conjugate gradient (PCG) solver. Let us define $B_\Gamma := \begin{pmatrix} B_\Delta^{(k)} & B_\Pi^{(k)} \end{pmatrix} = \begin{pmatrix} B_\Delta^{(k)} & 0 \end{pmatrix}$ and $B_\Gamma = (B_\Gamma^{(1)}, \ldots, B_\Gamma^{(K)})$. The preconditioner for the PCG method is the scaled Dirichlet preconditioner M_{sD} defined by

$$M_{\mathrm{sD}} := B_\Gamma D^{-1} S D^{-1} B_\Gamma^\top,$$

where $S = \mathrm{diag}(S^{(1)}, \ldots, S^{(K)})$ with

$$S^{(k)} := \begin{pmatrix} A_{\Delta\Delta}^{(k)} & A_{\Delta\Pi}^{(k)} \\ A_{\Pi\Delta}^{(k)} & A_{\Pi\Pi}^{(k)} \end{pmatrix} - \begin{pmatrix} A_{\Delta\mathrm{I}}^{(k)} \\ A_{\Pi\mathrm{I}}^{(k)} \end{pmatrix} (A_{\Pi}^{(k)})^{-1} \begin{pmatrix} A_{\mathrm{I}\Delta}^{(k)} & A_{\mathrm{I}\Pi}^{(k)} \end{pmatrix}$$

is the restriction of the overall operator A to the skeleton and $D = \mathrm{diag}(D^{(1)}, \ldots, D^{(K)})$ is a diagonal matrix defined based on the principle of coefficient scaling: Each coefficient $d_{i,i}^{(k)}$ of $D^{(k)}$ is assigned

$$d_{i,i}^{(k)} := \frac{\alpha_k + \alpha_\ell}{\alpha_\ell}$$

for degree of freedom i associated to the interface $\Gamma^{(k,\ell)}$. If i corresponds to a primal degree of freedom, then ℓ can be chosen arbitrarily among the indices of the neighboring patches.

After solving the system (9), the solution vectors $\widetilde{\underline{u}}$ and $\underline{u}_\Pi$ and, finally, $\underline{u}$ are computed from $\underline{u}$ by means of simple patch-local postprocessing steps.

The execution of the IETI-DP method for the dG discretization described above requires basically the same computational steps as the IETI-DP method for dG discretizations on conforming patch decompositions, see [26, Section 3] for the detailed outline of the algorithm.

4.6 Condition number estimate

The following theorem allows to estimate the maximum number of iterations that the PCG solver with scaled Dirichlet preconditioner needs to reach a desired error tolerance. The condition number (and thus the number of iterations) depends on the patch sizes, the grid size and on the spline degrees as explicitly stated in the theorem (the constant C does not depend on these quantities). The dependence on the grid sizes and patch sizes is as expected for FETI-like methods. Moreover, the dependence on gird and patch sizes and spline degree is the same as for the continuous case in IgA,

see [25]. The condition number bound is independent of the diffusion parameters α_k, of the number of patches K, of the continuity of the spline spaces, and of the choice of the penalty parameter δ (provided δ is large enough such that the overall bilinear form is coercive). The constant C (and thus the condition number) also depends on the bounds for the geometry function, on the number of patches that meet in a vertex and the quasi uniformity of the grids.

Theorem 4.2. *Provided that the IETI-DP solver is set up as outlined in the previous sections,*

- *there is a constant $C_1 > 0$ such that*

$$\sup_{x \in \overline{\widehat{\Omega}}} \|\nabla G_k(x)\|_{\ell^2} \leq C_1 \, H_k \quad \textit{and} \quad \sup_{x \in \overline{\widehat{\Omega}}} \|(\nabla G_k(x))^{-1}\|_{\ell^2} \leq C_1 \, \frac{1}{H_k}$$

  for all $k = 1, \ldots, K$, where $H_k := \operatorname{diam}(\Omega^{(k)})$,

- *there is a constant $C_2 > 0$ such that*

$$|\{k \,:\, \mathbf{x} \in \partial\Omega^{(k)}, k = 1, \ldots, K\}| \leq C_2 \tag{11}$$

  holds for all vertices $\mathbf{x}$,

- *there is a constant $C_3 > 0$ such that*

$$C_3 H_k \leq |\Gamma^{(k,\ell)}| \tag{12}$$

  holds for all $k = 1, \ldots, K$ and all $\ell \in \mathcal{N}_\Gamma(k)$,

- *and the grids are quasi-uniform, i.e., there is a constant $C_4 > 0$ such that*

$$\widehat{h}_k \leq C_4 \, \widehat{h}_{\min,k}$$

  holds for all $k = 1, \ldots, K$,

then the condition number of the preconditioned system satisfies

$$\kappa(M_{\mathrm{sD}} F) \leq C \, p \, \left(1 + \log p + \max_{k=1,\ldots,K} \log \frac{H_k}{h_k}\right)^2$$

the constant C only depends on the constants C_1, C_2, C_3 and C_4.

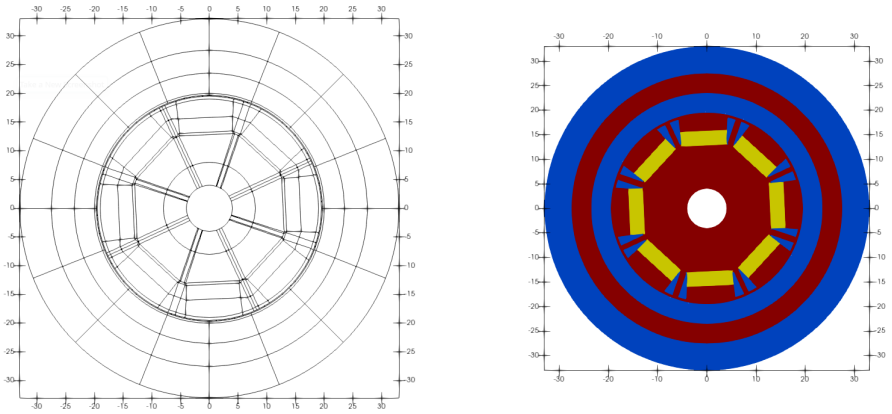

Figure 7: Decomposition of cross section into patches (left), and their materials (right)

5 Numerical results

In this section, we apply the IETI-DP method to a simple magnetostatic problem. We consider the computational domain shown in Figure 7 consisting of 272 patches representing a simplified cross section of an interior permanent magnet electric motor (IPMEM). The different colors in Fig. 7 denote different materials. The redbrown patches denote ferromagnetic material, e.g., iron, the yellow patches are the permanent magnets and the blue patches represent air regions and coils made of copper (for which we use the same material parameters).

The considered boundary reads formally as follows. Find u such that

$$\begin{aligned} -\mathrm{div}(\nu(x,y)\nabla u(x,y)) &= \mathrm{div}(\nu(x,y)M(x,y)) && \text{for} \quad (x,y)\in\Omega \\ u &= 0 && \text{on} \quad \partial\Omega, \end{aligned}$$

where ν denotes the magnetic reluctivity and M denotes the magnetization. The magnetic reluctivity is $\nu_{\text{ferro}} = \frac{1}{204\pi}10^5$ on the ferromagnetic parts, $\nu_{\text{mag}} = \frac{1}{4.344\pi}10^7$ on the permanent magnets and $\nu_{\text{air}} = \frac{1}{4\pi}10^7$ on the air and copper regions. This means that we have a jump in the order of approximately 10^4. On each of the permanent magnets, the magnetization M is given by

$$M = \rho_{\text{mag}}\,\nu_{\text{mag}}\,\mathbf{n},$$

where $\rho_{\text{mag}} := 1.28$ is the magnetic remanence, and $\mathbf{n}$ is unit the normal vector in positive or negative radial direction (measured from the center of the magnet), where a positive sign is used for every second magnet and a negative sign for every other second magnet. The magnetization M vanishes on the remainder of the domain (ferromagnetic parts, air, copper).

The cross section of the motor is modeled with NURBS and B-splines. For the coarsest discretization space, i.e., $r = 0$, we use B-splines that are global polynomials and we use only splines of maximum smoothness within the patches. The subsequent refinements

	$p=2$		$p=3$		$p=4$		$p=5$		$p=6$		$p=7$	
r	it	κ	it	κ	it	κ	it	κ	it	κ	it	κ
1	26	20.57	27	20.46	27	21.48	29	24.07	30	24.90	31	27.00
2	28	20.78	28	23.13	30	25.07	30	26.89	31	28.02	33	29.69
3	32	24.69	33	27.46	34	29.43	33	30.83	32	31.78	34	33.23
4	43	71.05	43	64.84	44	57.24	42	49.15	41	42.82	41	39.25
5	47	86.98	48	87.11	47	83.64	48	79.40	47	76.21	47	70.17
6	50	97.84	51	99.09	50	94.94	50	96.83	52	93.96	51	91.89

Table 1: Iterations (it) and condition numbers (κ); rotation angle of $\frac{5}{36}\pi$

$r = 1, 2, 3, \ldots$ are obtained via uniform refinement steps. We solve the IETI-DP system (9) with the M_{sD} preconditioner that arises from the magnetostatic model problem with a PCG solver and start the iterations with zero initial vector. We stop the iteration if the ℓ_2-norm of the residual has been decreased by a factor of 10^{-6} compared to the ℓ_2-norm of the right-hand side. We use the penalty parameter $\delta = 12$ for all the numerical experiments which are carried out on the Radon1[1] cluster located in Linz and we used the C++ library G+Smo [22].

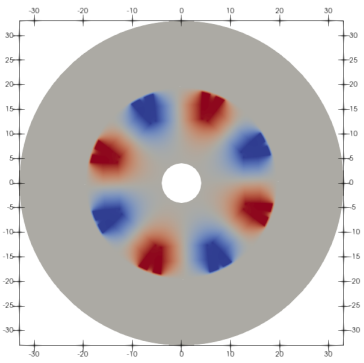

Figure 8: Solution of the linear model problem

Figure 8 shows a typical solution to the problem.

Table 1 shows the condition numbers and the iteration counts for the magnetostatic model problem. We see in this table a condition number growth with respect to h as expected and we also see that the condition numbers decrease for higher polynomial degrees from refinement level 4 on.

Table 2 reports on the robustness of the IETI-DP solver with respect to coefficient jumps. For the numerical tests we assign to the ferromagnetic patches the hypothetical

[1] https://www.ricam.oeaw.ac.at/hpc/

	$p=2$		$p=3$		$p=4$		$p=5$		$p=6$		$p=7$	
j	it	κ	it	κ	it	κ	it	κ	it	κ	it	κ
0	51	88.85	50	87.86	50	81.78	48	79.22	48	73.44	49	71.84
1	48	89.63	47	83.90	47	81.45	47	78.33	48	76.15	47	69.27
2	47	82.00	47	86.48	47	83.74	47	79.03	47	74.39	47	70.85
3	48	87.90	49	84.83	48	81.92	48	79.21	47	75.37	47	70.57
4	48	81.66	49	82.12	49	80.32	48	77.07	48	72.57	47	67.99

Table 2: Iterations (it) and condition numbers (κ); ν-robustness

	$p=3$		$p=4$		$p=5$		$p=6$		$p=7$		
r	it	κ	it	κ	it	κ	it	κ	it	κ	φ
4	43	64.84	44	57.24	42	49.15	41	42.82	41	39.25	$\frac{5}{36}\pi$
5	48	87.11	47	83.64	48	79.40	47	76.21	47	70.17	
6	51	99.09	50	94.94	50	96.83	52	93.96	51	91.89	
4	37	33.77	37	34.14	37	35.33	38	36.48	38	37.55	$\frac{6}{36}\pi$
5	43	55.63	43	52.20	42	49.48	42	46.78	42	45.63	
6	44	61.54	44	59.93	44	59.64	46	58.46	45	56.42	
4	36	31.88	37	33.66	37	35.01	37	36.23	38	37.60	$\frac{7}{36}\pi$
5	39	36.89	40	38.35	39	39.50	39	40.56	40	41.68	
6	41	41.82	41	42.96	41	44.30	42	45.45	42	46.55	

Table 3: Iteration counts (it) and condition numbers (κ); rotation dependence

reluctivity 10^{j} for $r = 5$ refinement steps. We see in the table that the condition number is almost independent of the coefficient jumps.

In Table 3, we see the dependence of the iteration and condition numbers with respect to the angle of rotation of the motor. We choose three different angle positions φ at $\frac{5}{36}\pi$, $\frac{6}{36}\pi$ and $\frac{7}{36}\pi$. We observe from this table that the iterations and condition numbers decrease for a larger angle φ.

The Table 4 shows the solving times in seconds (sec.) required to solve the IETI-DP system with the number of computing cores given in the column proc. We increase the number of cores from 2 to 16. We see in this table a very good scaling behavior of the algorithm.

proc	r	$p=3$ time	$p=4$ time	$p=5$ time	$p=6$ time	$p=7$ time
2	4	8.33	10.97	11.78	13.23	16.67
4	4	4.26	5.62	6.09	6.85	8.57
8	4	2.14	2.89	3.07	3.59	4.40
16	4	1.09	1.46	1.58	1.87	2.23
2	5	34.46	44.5	58.43	74.14	93.90
4	5	17.57	23.08	29.84	38.27	48.52
8	5	8.91	12.19	15.72	19.93	25.32
16	5	4.57	6.29	7.90	10.08	12.86
2	6	179.23	231.30	327.64	403.44	453.04
4	6	91.35	119.14	165.17	203.06	232.80
8	6	47.03	61.67	87.27	104.03	120.06
16	6	23.93	31.27	45.38	53.73	61.79
2	7	990.49	1356.09	1681.87	2692.77	OoM
4	7	499.52	700.10	873.77	1390.72	1567.99
8	7	257.08	364.11	443.77	720.69	809.26
16	7	129.83	190.08	227.36	366.35	413.41

Table 4: Time in seconds to solve (9)

6 Conclusions

In this paper, we have constructed a IETI-DP algorithm for computational domains with a non-matching decomposition into patches. We have adapted the idea of using corner values as primal degrees of freedom (Alg. A) from [26] according to our requirements. In this paper, we have generalized this idea to T-junctions: We add basis functions that are supported on a vertex to the primal space. For this choice, we obtain the same h and p-explicit condition number bounds as in [26].

A Appendix

In the appendix, we give a proof of Theorem 4.2. Throughout this appendix, we use the notation $a \lesssim b$ if there is a constant $c > 0$ that only depends on the constants C_1, C_2, C_3 and C_4 from Theorem 4.2 such that $a \leq cb$. Moreover, we write $a \eqsim b$ if $a \lesssim b \lesssim a$.

When it is clear from the context, we do not denote the restriction of a function to an interface explicitly, so we write for example $\|u^{(k)}\|_{L_2(\Gamma^{(k,\ell)})}$ instead of $\|u^{(k)}|_{\Gamma^{(k,\ell)}}\|_{L_2(\Gamma^{(k,\ell)})}$.

Following the usual approach, for the analysis, we need to introduce the skeleton representation of the solution which is obtained by eliminating the interior degrees of freedom. By eliminating the interior degrees of freedom from the spaces $V^{(k)}$, we obtain the space $W^{(k)} := \{v|_{\partial\Omega^{(k)}} : v \in V^{(k)}\}$. The introduction of the skeleton representation has no influence on the function spaces on the artificial interfaces, thus we define $W^{(k,\ell)} := V^{(k,\ell)}$. Based on these choices, we define analogously to V and $V_e^{(k)}$ the function spaces

$$W := W_e^{(1)} \times \cdots \times W_e^{(K)}, \quad \text{and} \quad W_e^{(k)} := W^{(k)} \times \prod_{\ell \in \mathcal{N}_\Gamma(k)} W^{(k,\ell)}.$$

Analogously to (6), a function $w_e^{(k)} \in W_e^{(k)}$ has the form $w_e^{(k)} = \left(w^{(k)}, \left(w^{(k,\ell)}\right)_{\ell \in \mathcal{N}_\Gamma(k)}\right)$, where $w^{(k)} \in W^{(k)}$ and $w^{(k,\ell)} \in W^{(k,\ell)}$. A basis for $W_e^{(k)}$ is canonically defined by choosing the traces of the basis functions of the basis of $V^{(k)}$ (for which the trace does not vanish) and the basis functions of the bases of $V^{(k,\ell)} = W^{(k,\ell)}$. Finally $\widetilde{W} \subseteq W$ is the subspace of functions where the primal constraints are satisfied, i.e., the coefficients for the vertex basis functions agree.

As in [25], we define the seminorm

$$|v|_{L_\infty^0(T)} := \inf_{c \in \mathbb{R}} \|v - c\|_{L_\infty(T)}$$

for a continuous function v over the set $T \subset \mathbb{R}^2$. Moreover, we use the standard seminorm

$$|v|_{H^{1/2}(T)} := \int_T \int_T \frac{(v(x) - v(y))^2}{\|x - y\|_{\ell^2}^2} \, \mathrm{d}y \, \mathrm{d}x$$

for T being the boundary or an edge of a patch.

The following lemma allows to estimate the action of the matrix $B_D^\top B_\Gamma$, where we define $B_D := B_\Gamma D^{-1}$.

Lemma A.1. *Let $u = (u_e^{(1)}, \cdots, u_e^{(K)}) = ((u^{(1)}, (u^{(1,\ell)})_{\ell \in \mathcal{N}_\Gamma(1)}), \ldots) \in \widetilde{W}$ with coefficient vector $\underline{u}$ and let $w = (w_e^{(1)}, \cdots, w_e^{(K)}) = ((w^{(1)}, (w^{(1,\ell)})_{\ell \in \mathcal{N}_\Gamma(1)}), \ldots) \in \widetilde{W}$ with coefficient vector $\underline{w}$ be such that $\underline{w} = B_D^\top B_\Gamma \underline{u}$. Then, we have for each patch $\Omega^{(k)}$ and each interface $\Gamma^{(k,\ell)}$ that*

$$w^{(k)}|_{\Gamma^{(k,\ell)}} = \frac{\alpha_\ell}{\alpha_k + \alpha_\ell}(u^{(k)}|_{\Gamma^{(k,\ell)}} - u^{(\ell,k)}), \quad w^{(k,\ell)} = \frac{\alpha_\ell}{\alpha_k + \alpha_\ell}(u^{(k,\ell)} - u^{(\ell)}|_{\Gamma^{(k,\ell)}}).$$

Proof. As in the proof of [26, Lemma 4.3], we have

$$
\begin{aligned}
w^{(k)}|_{\Gamma^{(k,\ell)}} &= \frac{\alpha_\ell}{\alpha_k+\alpha_\ell} \\
&\qquad \left(u^{(k)}|_{\Gamma^{(k,\ell)}} - u^{(\ell,k)} - \sum_{T\in\Gamma^{(k,\ell)}} \sum_{(i,j)\in\mathcal{B}_T(k,\ell)} \left(u_i^{(k)}\varphi_i^{(k)}|_{\Gamma^{(k,\ell)}} - u_j^{(\ell,k)}\varphi_j^{(\ell,k)} \right) \right), \\
w^{(k,\ell)}|_{\Gamma^{(k,\ell)}} &= \frac{\alpha_\ell}{\alpha_k+\alpha_\ell} \\
&\qquad \left(u^{(k,\ell)} - u^{(\ell)}|_{\Gamma^{(k,\ell)}} - \sum_{T\in\Gamma^{(k,\ell)}} \sum_{(i,j)\in\mathcal{B}_T(\ell,k)} \left(u_i^{(k,\ell)}\varphi_i^{(k,\ell)} - u_j^{(\ell)}\varphi_j^{(\ell)}|_{\Gamma^{(k,\ell)}} \right) \right),
\end{aligned}
\tag{13}
$$

where $\varphi_i^{(k)}$ denotes a basis function of the basis of $W^{(k)}$ and $\varphi_i^{(k,\ell)}$ denotes a basis function of the basis of $W^{(k,\ell)}$. The set $\mathcal{B}_T(k,\ell)$ contains the pairs of indices of those basis functions in the bases for $W^{(k)}$ and $W^{(\ell,k)}$ which are subject to a primal constraint.

We obtain the representation (13) since the coefficients corresponding to all basis functions on the common edge $\Gamma^{(k,\ell)}$ are equal to $\pm\alpha_\ell/(\alpha_k+\alpha_\ell)$, except to the basis functions that correspond to the primal degrees of freedom. For the latter, the corresponding coefficients are 0 since the primal degrees of freedoms are not subject to the jump matrix. Thus, we subtract the latter.

Note that $u \in \widetilde{W}$, which means that it satisfies the primal constraints. Hence the sum over the indices in $\mathcal{B}_T(k,\ell)$ vanishes. Therefore, we immediately obtain the desired result. □

Lemma A.1 and the triangle inequality immediately yield

$$
\begin{aligned}
\|w^{(k)} - w^{(k,\ell)}\|^2_{L_2(\Gamma^{(k,\ell)})} &\lesssim \frac{\alpha_\ell^2}{(\alpha_k+\alpha_\ell)^2} \left(\|u^{(k)} - u^{(k,\ell)}\|^2_{L_2(\Gamma^{(k,\ell)})} + \|u^{(\ell)} - u^{(\ell,k)}\|^2_{L_2(\Gamma^{(k,\ell)})} \right), \\
|w^{(k)}|^2_{H^{1/2}(\Gamma^{(k,\ell)})} &\lesssim \frac{\alpha_\ell^2}{(\alpha_k+\alpha_\ell)^2} \left(|u^{(k)}|^2_{H^{1/2}(\Gamma^{(k,\ell)})} + |u^{(\ell,k)}|^2_{H^{1/2}(\Gamma^{(k,\ell)})} \right), \\
|w^{(k)}|^2_{L^0_\infty(\Gamma^{(k,\ell)})} &\lesssim \frac{\alpha_\ell^2}{(\alpha_k+\alpha_\ell)^2} \left(|u^{(k)}|^2_{L^0_\infty(\Gamma^{(k,\ell)})} + |u^{(\ell,k)}|^2_{L^0_\infty(\Gamma^{(k,\ell)})} \right).
\end{aligned}
\tag{14}
$$

Here and in what follows, we write $\widehat{h}_{k\ell} := \min\{\widehat{h}_k, \widehat{h}_\ell\}$ and $h_{k\ell} := \min\{h_k, h_\ell\}$.

We estimate contributions from the artificial interfaces in the $H^{1/2}$- and L^0_∞-seminorms. We start with the $H^{1/2}$ estimate.

Lemma A.2. *Let $u \in \widetilde{W}$. Then, the estimate*

$$
|u^{(k,\ell)}|^2_{H^{1/2}(\Gamma^{(k,\ell)})} \lesssim |u^{(k)}|^2_{H^{1/2}(\partial\Omega^{(k)})} + |u^{(\ell)}|^2_{H^{1/2}(\partial\Omega^{(\ell)})} + \frac{p^2}{h_{k\ell}} \|u^{(k,\ell)} - u^{(k)}\|^2_{L_2(\Gamma^{(k,\ell)})}
$$

holds.

Proof. The triangle inequality yields

$$|u^{(k,\ell)}|^2_{H^{1/2}(\Gamma^{(k,\ell)})} \leq 2|u^{(k)}|^2_{H^{1/2}(\Gamma^{(k,\ell)})} + 2|u^{(k)} - u^{(k,\ell)}|^2_{H^{1/2}(\Gamma^{(k,\ell)})}. \tag{15}$$

To estimate $|u^{(k)} - u^{(k,\ell)}|_{H^{1/2}(\Gamma^{(k,\ell)})}$, we use the equivalence of the norms on the physical and the parameter domain, [26, Lemma 1], and interpolation, cf. [1, Theorem 5.2, eq. (3)], to obtain

$$\begin{aligned}
|u^{(k)} - u^{(k,\ell)}|^2_{H^{1/2}(\Gamma^{(k,\ell)})} &\eqsim |\widehat{u}^{(k)} - \widehat{u}^{(k,\ell)}|^2_{H^{1/2}(\widehat{\Gamma}^{(k,\ell)})} \\
&\lesssim \|\widehat{u}^{(k)} - \widehat{u}^{(k,\ell)}\|_{L_2(\widehat{\Gamma}^{(k,\ell)})} \|\widehat{u}^{(k)} - \widehat{u}^{(k,\ell)}\|_{H^1(\widehat{\Gamma}^{(k,\ell)})} \\
&\eqsim \|\widehat{u}^{(k)} - \widehat{u}^{(k,\ell)}\|^2_{L_2(\widehat{\Gamma}^{(k,\ell)})} + \|\widehat{u}^{(k)} - \widehat{u}^{(k,\ell)}\|_{L_2(\widehat{\Gamma}^{(k,\ell)})} |\widehat{u}^{(k)} - \widehat{u}^{(k,\ell)}|_{H^1(\widehat{\Gamma}^{(k,\ell)})} \\
&\leq \frac{p^2}{\widehat{h}_{k\ell}} \|\widehat{u}^{(k)} - \widehat{u}^{(k,\ell)}\|^2_{L_2(\widehat{\Gamma}^{(k,\ell)})} + \|\widehat{u}^{(k)} - \widehat{u}^{(k,\ell)}\|_{L_2(\widehat{\Gamma}^{(k,\ell)})} |\widehat{u}^{(k)} - \widehat{u}^{(k,\ell)}|_{H^1(\widehat{\Gamma}^{(k,\ell)})}.
\end{aligned} \tag{16}$$

Next, we rotate the patches such that $\widehat{\Gamma}^{(k,\ell)}$ is $(a_1, a_2) \times \{0\}$. We define the function $\widetilde{u}^{(k,\ell)} := \widehat{u}^{(k,\ell)}(\cdot, 0)$ and we denote by $\widetilde{\zeta}_1$ and $\widetilde{\zeta}_2$ the smallest and largest breakpoints, respectively, corresponding to the basis $\widehat{\Phi}^{(k,\ell)}$ such that $\widetilde{\zeta}_1 \geq a_1$ and $\widetilde{\zeta}_2 \leq a_2$. Using the triangle inequality, we estimate $|\widehat{u}^{(k)} - \widehat{u}^{(k,\ell)}|_{H^1(\widehat{\Gamma}^{(k,\ell)})}$ as

$$\begin{aligned}
&|\widehat{u}^{(k)} - \widehat{u}^{(k,\ell)}|_{H^1(\widehat{\Gamma}^{(k,\ell)})} \\
&\quad\lesssim |\widehat{u}^{(k)}|_{H^1(\widehat{\Gamma}^{(k,\ell)})} + |\widetilde{u}^{(k,\ell)}|_{H^1((a_1,a_2))} \\
&\quad\lesssim |\widehat{u}^{(k)}|_{H^1(\widehat{\Gamma}^{(k,\ell)})} + |\widetilde{u}^{(k,\ell)}|_{H^1((\widetilde{\zeta}_1,\widetilde{\zeta}_2))} + |\widetilde{u}^{(k,\ell)}|_{H^1((a_1,a_2)\setminus(\widetilde{\zeta}_1,\widetilde{\zeta}_2))}.
\end{aligned}$$

On $(\widetilde{\zeta}_1, \widetilde{\zeta}_2)$, we use [12, Proposition 2.2] and apply an inverse inequality of [25, Lemma 4.3]. On $(a_1, a_2)\setminus(\widetilde{\zeta}_1, \widetilde{\zeta}_2)$, we use the fact that $u \in \widetilde{W}$. Hence, $\widetilde{u}^{(k,\ell)} = \widetilde{u}^{(\ell)}$ on $(a_1, a_2)\setminus(\widetilde{\zeta}_1, \widetilde{\zeta}_2)$ and we estimate

$$\begin{aligned}
&|\widehat{u}^{(k)} - \widehat{u}^{(k,\ell)}|_{H^1(\widehat{\Gamma}^{(k,\ell)})} \\
&\quad\lesssim |\widehat{u}^{(k)}|_{H^1(\partial\widehat{\Omega})} + \frac{p}{(\widehat{h}_{k\ell})^{1/2}} |\widehat{u}^{(k,\ell)}|_{H^{1/2}(\widehat{\Gamma}^{(k,\ell)}))} + |\widehat{u}^{(\ell)}|_{H^1(\partial\widehat{\Omega})} \\
&\quad\lesssim \frac{p}{(\widehat{h}_{k\ell})^{1/2}} \left(|\widehat{u}^{(k)}|_{H^{1/2}(\partial\widehat{\Omega})} + |\widehat{u}^{(k,\ell)}|_{H^{1/2}(\widehat{\Gamma}^{(k,\ell)}))} + |\widehat{u}^{(\ell)}|_{H^{1/2}(\partial\widehat{\Omega})} \right).
\end{aligned} \tag{17}$$

We insert (17) into (16) and further into (15), apply the norm equivalence between the parameter and physical domain, [26, Lemma 1], and denote by $c_1, c_2 > 0$ the hidden constants in the estimate to get

$$\begin{aligned}
|u^{(k,\ell)}|^2_{H^{1/2}(\Gamma^{(k,\ell)})} \leq 2|u^{(k)}|^2_{H^{1/2}(\Gamma^{(k,\ell)})} &+ \frac{c_1 p^2}{h_{k\ell}} \|u^{(k)} - u^{(k,\ell)}\|^2_{L_2(\Gamma^{(k,\ell)})} \\
&+ \frac{c_2 p}{(h_{k\ell})^{1/2}} \|u^{(k)} - u^{(k,\ell)}\|_{L_2(\Gamma^{(k,\ell)})} \\
&\left(|u^{(k)}|_{H^{1/2}(\partial\Omega^{(k)})} + |u^{(k,\ell)}|_{H^{1/2}(\Gamma^{(k,\ell)})} + |u^{(\ell)}|_{H^{1/2}(\partial\Omega^{(\ell)})} \right).
\end{aligned}$$

Using $ab \le a^2 + b^2/4$ and $(a+b)^2 \le 2a^2 + 2b^2$, we obtain

$$|u^{(k,\ell)}|^2_{H^{1/2}(\Gamma^{(k,\ell)})} \le 2|u^{(k)}|^2_{H^{1/2}(\Gamma^{(k,\ell)})} + \frac{(c_1+c_2^2)p^2}{h_{k\ell}}\|u^{(k)} - u^{(k,\ell)}\|^2_{L_2(\Gamma^{(k,\ell)})} + \frac{1}{2}|u^{(k,\ell)}|^2_{H^{1/2}(\Gamma^{(k,\ell)})} + |u^{(k)}|^2_{H^{1/2}(\partial\Omega^{(k)})} + |u^{(\ell)}|^2_{H^{1/2}(\partial\Omega^{(\ell)})}.$$

We subtract $\frac{1}{2}|u^{(k,\ell)}|^2_{H^{1/2}(\Gamma^{(k,\ell)})}$ from the equation to get statement of the lemma. □

Lemma A.3. *Let $u \in \widetilde{W}$. Then,*

$$|u^{(k,\ell)}|^2_{L^0_\infty(\Gamma^{(k,\ell)})} \lesssim |u^{(k)}|^2_{L^0_\infty(\Gamma^{(k,\ell)})} + |u^{(k)}|^2_{H^{1/2}(\partial\Omega^{(k)})} + |u^{(\ell)}|^2_{H^{1/2}(\partial\Omega^{(\ell)})} + \frac{p^2}{h_{k\ell}}\|u^{(k)} - u^{(k,\ell)}\|^2_{L_2(\Gamma^{(k,\ell)})}$$

holds.

Proof. Using the triangle inequality, we obtain

$$|u^{(k,\ell)}|^2_{L^0_\infty(\Gamma^{(k,\ell)})} \lesssim |u^{(k)}|^2_{L^0_\infty(\Gamma^{(k,\ell)})} + |u^{(k)} - u^{(k,\ell)}|^2_{L^0_\infty(\Gamma^{(k,\ell)})}. \tag{18}$$

We apply [26, Lemma 5] and the norm equivalence, [26, Lemma 1], to the difference $|u^{(k)} - u^{(k,\ell)}|^2_{L^0_\infty(\Gamma^{(k,\ell)})}$ to get

$$\begin{aligned}
|u^{(k)} - u^{(k,\ell)}|^2_{L^0_\infty(\Gamma^{(k,\ell)})} &= |\widehat{u}^{(k)} - \widehat{u}^{(k,\ell)}|^2_{L^0_\infty(\widehat{\Gamma}^{(k,\ell)})} \\
&\lesssim \|\widehat{u}^{(k)} - \widehat{u}^{(k,\ell)}\|_{L_2(\widehat{\Gamma}^{(k,\ell)})}\|\widehat{u}^{(k)} - \widehat{u}^{(k,\ell)}\|_{H^1(\widehat{\Gamma}^{(k,\ell)})} \\
&\lesssim \|\widehat{u}^{(k)} - \widehat{u}^{(k,\ell)}\|^2_{L_2(\widehat{\Gamma}^{(k,\ell)})} + \|\widehat{u}^{(k)} - \widehat{u}^{(k,\ell)}\|_{L_2(\widehat{\Gamma}^{(k,\ell)})}|\widehat{u}^{(k)} - \widehat{u}^{(k,\ell)}|_{H^1(\widehat{\Gamma}^{(k,\ell)})} \\
&\le \frac{p^2}{\widehat{h}_{k\ell}}\|\widehat{u}^{(k)} - \widehat{u}^{(k,\ell)}\|^2_{L_2(\widehat{\Gamma}^{(k,\ell)})} + \|\widehat{u}^{(k)} - \widehat{u}^{(k,\ell)}\|_{L_2(\widehat{\Gamma}^{(k,\ell)})}|\widehat{u}^{(k)} - \widehat{u}^{(k,\ell)}|_{H^1(\widehat{\Gamma}^{(k,\ell)})}.
\end{aligned}$$

We use (17) to obtain

$$|\widehat{u}^{(k)} - \widehat{u}^{(k,\ell)}|_{H^1(\widehat{\Gamma}^{(k,\ell)})} \lesssim \frac{p}{(\widehat{h}_{k\ell})^{1/2}}\left(|\widehat{u}^{(k)}|_{H^{1/2}(\partial\widehat{\Omega})} + |\widehat{u}^{(k,\ell)}|_{H^{1/2}(\widehat{\Gamma}^{(k,\ell)})} + |\widehat{u}^{(\ell)}|_{H^{1/2}(\partial\widehat{\Omega})}\right).$$

An application of the norm equivalence, [26, Lemma 1], yields the estimate

$$|u^{(k)} - u^{(k,\ell)}|^2_{L^0_\infty(\Gamma^{(k,\ell)})} \lesssim \frac{p^2}{h_{k\ell}}\|u^{(k)} - u^{(k,\ell)}\|^2_{L_2(\Gamma^{(k,\ell)})} + \frac{p}{(h_{k\ell})^{1/2}}\|u^{(k)} - u^{(k,\ell)}\|_{L_2(\Gamma^{(k,\ell)})} \left(|u^{(k)}|_{H^{1/2}(\partial\Omega^{(k)})} + |u^{(k,\ell)}|_{H^{1/2}(\Gamma^{(k,\ell)})} + |u^{(\ell)}|_{H^{1/2}(\partial\Omega^{(\ell)})}\right).$$

Using $a(b+c) \lesssim a^2 + b^2 + c^2$ and $(a+b)^2 \lesssim a^2 + b^2$, yield

$$|u^{(k)} - u^{(k,\ell)}|^2_{L^0_\infty(\Gamma^{(k,\ell)})} \lesssim \frac{p^2}{h_{k\ell}}\|u^{(k)} - u^{(k,\ell)}\|^2_{L_2(\Gamma^{(k,\ell)})} + |u^{(k)}|^2_{H^{1/2}(\partial\Omega^{(k)})} + |u^{(k,\ell)}|^2_{H^{1/2}(\Gamma^{(k,\ell)})} + |u^{(\ell)}|^2_{H^{1/2}(\partial\Omega^{(\ell)})}.$$

Lemma A.2 and (18) finish the proof of this lemma. □

Before we give a proof of the main theorem, we estimate the sum of the corresponding seminorms over all patches.

Lemma A.4. *Let u and w be as in Lemma A.1 and assume that* (11) *holds. Then, we have*

$$\sum_{k=1}^{K}\sum_{\ell\in\mathcal{N}_\Gamma(k)}\alpha_k\left(|w^{(k)}|^2_{H^{1/2}(\Gamma^{(k,\ell)})}+|w^{(k)}|^2_{L^0_\infty(\Gamma^{(k,\ell)})}\right)$$
$$\lesssim\sum_{k=1}^{K}\sum_{\ell\in\mathcal{N}_\Gamma(k)}\alpha_k\left(|u^{(k)}|^2_{H^{1/2}(\partial\Omega^{(k)})}+|u^{(k)}|^2_{L^0_\infty(\Gamma^{(k,\ell)})}+\frac{p^2}{h_{k\ell}}\|u^{(k)}-u^{(k,\ell)}\|^2_{L_2(\Gamma^{(k,\ell)})}\right).$$

Proof. Within this proof, all norms refer to $\Gamma^{(k,\ell)}=\Gamma^{(\ell,k)}$. (14) and (11) yield

$$\mathcal{A}:=\sum_{k=1}^{K}\sum_{\ell\in\mathcal{N}_\Gamma(k)}\alpha_k\left(|w^{(k)}|^2_{H^{1/2}(\Gamma^{(k,\ell)})}+|w^{(k)}|^2_{L^0_\infty(\Gamma^{(k,\ell)})}\right)$$
$$\lesssim\sum_{k=1}^{K}\sum_{\ell\in\mathcal{N}_\Gamma(k)}\frac{\alpha_k\alpha_\ell^2}{(\alpha_k+\alpha_\ell)^2}\Big(|u^{(k)}|^2_{H^{1/2}(\Gamma^{(k,\ell)})}+|u^{(\ell,k)}|^2_{H^{1/2}(\Gamma^{(k,\ell)})}$$
$$+|u^{(k)}|^2_{L^0_\infty(\Gamma^{(k,\ell)})}+|u^{(\ell,k)}|^2_{L^0_\infty(\Gamma^{(k,\ell)})}\Big).$$

Using Lemmas A.2 and A.3, we obtain

$$\mathcal{A}\lesssim\sum_{k=1}^{K}\sum_{\ell\in\mathcal{N}_\Gamma(k)}\frac{\alpha_k\alpha_\ell^2}{(\alpha_k+\alpha_\ell)^2}\Big(|u^{(k)}|^2_{H^{1/2}(\partial\Omega^{(k)})}+|u^{(\ell)}|^2_{H^{1/2}(\partial\Omega^{(\ell)})}$$
$$+|u^{(k)}|^2_{L^0_\infty(\Gamma^{(k,\ell)})}+|u^{(\ell)}|^2_{L^0_\infty(\Gamma^{(k,\ell)})}+\frac{p^2}{h_{k\ell}}\|u^{(\ell)}-u^{(\ell,k)}\|^2_{L_2(\Gamma^{(k,\ell)})}\Big).$$

The estimate $\frac{\alpha_k\alpha_\ell^2}{(\alpha_k+\alpha_\ell)^2}\leq\min\{\alpha_k,\alpha_\ell\}$, and $\ell\in\mathcal{N}_\Gamma(k)\Leftrightarrow k\in\mathcal{N}_\Gamma(\ell)$ yield the desired estimate. □

Proof of Theorem 4.2. The idea of the proof is to use [21, Theorem 22], which states that

$$\kappa(M_{\mathrm{sD}}F)\leq\sup_{u\in\widetilde{W}}\frac{\|B_D^\top B_\Gamma\underline{u}\|_S^2}{\|\underline{u}\|_S^2},\tag{19}$$

where $\underline{u}$ is the coefficient vector associated to the function $u=(u_e^{(1)},\cdots,u_e^{(K)})=((u^{(1)},(u^{(1,\ell)})_{\ell\in\mathcal{N}_\Gamma(k)}),\cdots)$. So, let u be arbitrary but fixed and let the function $w=(w_e^{(1)},\cdots,w_e^{(K)})=((w^{(1)},(w^{(1,\ell)})_{\ell\in\mathcal{N}_\Gamma(k)}),\cdots)$ with coefficient vector $\underline{w}$ be such that $\underline{w}=B_D^\top B_\Gamma\underline{u}$. The Schur complement norm of the function w is equivalent to the dG norm of its discrete harmonic extension, cf. [26]. This means that

$$\|B_D^\top B_\Gamma\underline{u}\|_S^2=\|\underline{w}\|_S^2\eqsim\sum_{k=1}^{K}\alpha_k|\mathcal{H}_h^{(k)}w^{(k)}|^2_{H^1(\Omega^{(k)})}+\sum_{k=1}^{K}\sum_{\ell\in\mathcal{N}_\Gamma(k)}\alpha_k\frac{\delta p^2}{h_{kl}}\|w^{(k)}-w^{(k,\ell)}\|^2_{L_2(\Gamma^{(k,\ell)})},\tag{20}$$

where $\mathcal{H}_h^{(k)} : W^{(k)} \to V^{(k)}$ denotes the discrete harmonic extension that minimizes the energy with respect to the bilinear form $a^{(k)}(\cdot,\cdot)$. First, we estimate the first sum in (20). [25, Theorem 4.2] yields

$$\sum_{k=1}^{K} \alpha_k |\mathcal{H}_h^{(k)} w^{(k)}|^2_{H^1(\Omega^{(k)})} \lesssim p \sum_{k=1}^{K} \alpha_k |w^{(k)}|^2_{H^{1/2}(\partial\Omega^{(k)})}.$$

Using [25, Lemma 4.15] and an analogous estimate for a single edge (which depends on (12)), we get

$$\sum_{k=1}^{K} \alpha_k |\mathcal{H}_h^{(k)} w^{(k)}|^2_{H^1(\Omega^{(k)})} \lesssim p \sum_{k=1}^{K} \sum_{\ell\in\mathcal{N}_\Gamma(k)} \alpha_k \left(|w^{(k)}|^2_{H^{1/2}(\Gamma^{(k,\ell)})} + \Lambda |w^{(k)}|^2_{L^0_\infty(\Gamma^{(k,\ell)})} \right),$$

where $\Lambda := 1 + \log p + \max_{k=1,\dots,K} \log \frac{H_k}{h_k}$. Using $\Lambda \geq 1$ and Lemma A.4, we obtain further

$$\begin{aligned}\sum_{k=1}^{K} \alpha_k |\mathcal{H}_h^{(k)} w^{(k)}|^2_{H^1(\Omega^{(k)})} &\lesssim p\Lambda \sum_{k=1}^{K} \sum_{\ell\in\mathcal{N}_\Gamma(k)} \alpha_k \left(|u^{(k)}|^2_{H^{1/2}(\partial\Omega^{(k)})} + |u^{(k)}|^2_{L^0_\infty(\Gamma^{(k,\ell)})} \right) \\ &\quad + p\Lambda \sum_{k=1}^{K} \sum_{\ell\in\mathcal{N}_\Gamma(k)} \alpha_k \frac{p^2}{h_{k\ell}} \|u^{(k,\ell)} - u^{(k)}\|^2_{L_2(\Gamma^{(k,\ell)})}.\end{aligned}$$

Using [25, Lemma 4.15 and Theorem 4.2] and $|\mathcal{N}_\Gamma(k)| \lesssim 1$, we further estimate

$$\begin{aligned}\sum_{k=1}^{K} \alpha_k |\mathcal{H}_h^{(k)} w^{(k)}|^2_{H^1(\Omega^{(k)})} &\lesssim p\Lambda \sum_{k=1}^{K} \alpha_k |\mathcal{H}_h^{(k)} u^{(k)}|^2_{H^1(\Omega^{(k)})} + p\Lambda \sum_{k=1}^{K} \sum_{\ell\in\mathcal{N}_\Gamma(k)} \alpha_k |u^{(k)}|^2_{L^0_\infty(\Gamma^{(k,\ell)})} \\ &\quad + p\Lambda \sum_{k=1}^{K} \sum_{\ell\in\mathcal{N}_\Gamma(k)} \alpha_k \frac{p^2}{h_{k\ell}} \|u^{(k,\ell)} - u^{(k)}\|^2_{L_2(\Gamma^{(k,\ell)})}.\end{aligned}$$

Using [25, Lemma 4.14], we get further

$$\begin{aligned}\sum_{k=1}^{K} \alpha_k |\mathcal{H}_h^{(k)} w^{(k)}|^2_{H^1(\Omega^{(k)})} &\lesssim p\Lambda \sum_{k=1}^{K} \alpha_k |\mathcal{H}_h^{(k)} u^{(k)}|^2_{H^1(\Omega^{(k)})} \\ &\quad + p\Lambda^2 \sum_{k=1}^{K} \alpha_k \sum_{\ell\in\mathcal{N}_\Gamma(k)} \left(|\mathcal{H}_h^{(k)} u^{(k)}|^2_{H^1(\Omega^{(k)})} + \inf_{c\in\mathbb{R}} \|(\mathcal{H}_h^{(k)} u^{(k)} - c) \circ G_k\|^2_{H^1(\widehat{\Omega})} \right) \\ &\quad + p\Lambda \sum_{k=1}^{K} \sum_{\ell\in\mathcal{N}_\Gamma(k)} \alpha_k \frac{p^2}{h_{k\ell}} \|u^{(k,\ell)} - u^{(k)}\|^2_{L_2(\Gamma^{(k,\ell)})}.\end{aligned}$$

The assumption (11), the Poincaré inequality and the norm equivalence between the

parameter and the physical domain, [26, Lemma 1], yield the estimate

$$\begin{aligned}&\sum_{k=1}^{K}\alpha_k|\mathcal{H}_h^{(k)}w^{(k)}|^2_{H^1(\Omega^{(k)})}\\&\quad\lesssim p\Lambda^2\sum_{k=1}^{K}\left(\alpha_k|\mathcal{H}_h^{(k)}u^{(k)}|^2_{H^1(\Omega^{(k)})}+\sum_{\ell\in\mathcal{N}_\Gamma(k)}\alpha_k\frac{p^2}{h_{k\ell}}\|u^{(k,\ell)}-u^{(k)}\|^2_{L_2(\Gamma^{(k,\ell)})}\right).\end{aligned}\tag{21}$$

The estimate (14), $\frac{\alpha_k\alpha_\ell^2}{(\alpha_k+\alpha_\ell)^2}\le\min\{\alpha_k,\alpha_\ell\}$ and $\ell\in\mathcal{N}_\Gamma(k)\Leftrightarrow k\in\mathcal{N}_\Gamma(\ell)$ immediately yield for the second sum in (20),

$$\sum_{k=1}^{K}\sum_{\ell\in\mathcal{N}_\Gamma(k)}\alpha_k\frac{\delta p^2}{h_{k\ell}}\|w^{(k)}-w^{(k,\ell)}\|^2_{L_2(\Gamma^{(k,\ell)})}\lesssim\sum_{k=1}^{K}\sum_{\ell\in\mathcal{N}_\Gamma(k)}\alpha_k\frac{\delta p^2}{h_{k\ell}}\|u^{(k)}-u^{(k,\ell)}\|^2_{L_2(\Gamma^{(k,\ell)})}.\tag{22}$$

Using the fact that $\Lambda\ge1$, (21) and (22) to estimate (20), we obtain

$$\begin{aligned}\|B_D^\top B_\Gamma\underline{u}\|_S^2&\lesssim p\Lambda^2\sum_{k=1}^{K}\left(\alpha_k|\mathcal{H}_h^{(k)}u^{(k)}|^2_{H^1(\Omega^{(k)})}+\sum_{\ell\in\mathcal{N}_\Gamma(k)}\alpha_k\frac{\delta p^2}{h_{k\ell}}\|u^{(k)}-u^{(k,\ell)}\|^2_{L_2(\Gamma^{(k,\ell)})}\right)\\&=p\Lambda^2\|u\|_d^2\eqsim p\Lambda^2\|\underline{u}\|_S^2\end{aligned}$$

The combination of this estimate and (19) finishes the proof. □

Acknowledgments. The first author was supported by the Austrian Science Fund (FWF): S117 and W1214-04. Also, the second author has received support from the Austrian Science Fund (FWF): P31048.

References

[1] R. Adams and J. Fournier. *Sobolev Spaces.* Elsevier Science, 2003.

[2] P. Alotto, A. Bertoni, I. Perugia, and D. Schoetzau. Discontinuous finite element methods for the simulation of rotating electrical machines. *COMPEL*, 20:448 – 462, 2001.

[3] D. Arnold. An interior penalty finite element method with discontinuous elements. *SIAM J. Numer. Anal.*, 19(4):742 – 760, 1982.

[4] A. Buffa, Y. Maday, and F. Rapetti. A sliding mesh-mortar method for a two dimensional eddy currents model of electric engines. *ESAIM: Math. Model. Numer. Anal.*, 35(2):191 – 228, 2001.

[5] M. Cafiero, O. Lloberas-Valls, J. Cante, and J. Oliver. The domain interface method: a general-purpose non-intrusive technique for non-conforming domain decomposition problems. *Comput. Mech.*, 57(4):555 – 581, 2016.

[6] J. A. Cottrell, T. J. R. Hughes, and Y. Bazilevs. *Isogeometric Analysis – Toward Integration of CAD and FEA*. John Wiley & Sons, 2009.

[7] B. Davat, Z. Ren, and M. Lajoie-Mazenc. The movement in field modeling. *IEEE Trans. Magn.*, 21(6):2296 – 2298, 1985.

[8] M. Dryja, J. Galvis, and M. Sarkis. A FETI-DP preconditioner for a composite finite element and discontinuous Galerkin method. *SIAM J. Numer. Anal.*, 51(1):400 – 422, 2013.

[9] H. Egger, M. Harutyunyan, M. Merkel, and S. Schöps. On the stability of harmonic mortar methods with application to electric machines, 2020. `https://arxiv.org/pdf/2005.12020.pdf`.

[10] C. Farhat, M. Lesoinne, P. L. Tallec, K. Pierson, and D. Rixen. FETI-DP: A dual-primal unified FETI method I: A faster alternative to the two-level FETI method. *Int. J. Numer. Methods Eng.*, 50:1523 – 1544, 2001.

[11] C. Farhat and F.-X. Roux. A method of finite element tearing and interconnecting and its parallel solution algorithm. *Int. J. Numer. Methods Eng.*, 32(6):1205 – 1227, 1991.

[12] N. Heuer. On the equivalence of fractional-order Sobolev semi-norms. *J. Math. Anal. Appl.*, 417(2):505–518, 2014.

[13] C. Hofer. Analysis of discontinuous Galerkin dual-primal isogeometric tearing and interconnecting methods. *Math. Models Methods Appl. Sci.*, 28(1):131 – 158, 2018.

[14] C. Hofer and U. Langer. Dual-primal isogeometric tearing and interconnecting solvers for multipatch continuous and discontinuous Galerkin IgA equations. *PAMM*, 16(1):747 – 748, 2016.

[15] C. Hofer and U. Langer. Dual-primal isogeometric tearing and interconnecting solvers for multipatch dG-IgA equations. *Comput. Methods Appl. Mech. Eng.*, 316:2 – 21, 2017.

[16] C. Hofer, U. Langer, and I. Toulopoulos. Isogeometric analysis on non-matching segmentation: discontinuous Galerkin techniques and efficient solvers. *J. Appl. Math. Comput.*, 61(1):297 – 336, 2019.

[17] T. J. R. Hughes, J. A. Cottrell, and Y. Bazilevs. Isogeometric analysis: CAD, finite elements, NURBS, exact geometry and mesh refinement. *Comput. Methods Appl. Mech. Eng.*, 194(39-41):4135 – 4195, 2005.

[18] L. Kettunen, S. Kurz, T. Tarhasaari, V. Raisanen, A. Stenvall, and S. Suuriniemi. Modeling rotation in electrical machines. *IEEE Trans. Magn.*, 50(4):1 – 10, 2014.

[19] S. Kleiss, C. Pechstein, B. Jüttler, and S. Tomar. IETI-Isogeometric Tearing and Interconnecting. *Comput. Methods Appl. Mech. Eng.*, 247-248:201 – 215, 2012.

[20] H. C. Lai, D. Rodger, and P. J. Leonard. Coupling meshes in 3D problems involving movements. *IEEE Trans. Magn.*, 28(2):1732 – 1734, 1992.

[21] J. Mandel, C. R. Dohrmann, and R. Tezaur. An algebraic theory for primal and dual substructuring methods by constraints. *Appl. Numer. Math.*, 54(2):167 – 193, 2005.

[22] A. Mantzaflaris, R. Schneckenleitner, S. Takacs, and others (see website). G+Smo (Geometry plus Simulation modules). `http://github.com/gismo`, 2020.

[23] R. Perrin-Bit and J. L. Coulomb. A three dimensional finite element mesh connection for problems involving movement. *IEEE Trans. Magn.*, 31(3):1920 – 1923, 1995.

[24] T. W. Preston, A. B. J. Reece, and P. S. Sangha. Induction motor analysis by time-stepping techniques. *IEEE Trans. Magn.*, 24(1):471 – 474, 1988.

[25] R. Schneckenleitner and S. Takacs. Condition number bounds for IETI-DP methods that are explicit in h and p. *Math. Models Methods Appl. Sci.*, 30(11):2067 – 2103, 2020.

[26] R. Schneckenleitner and S. Takacs. Convergence theory for IETI-DP solvers for discontinuous Galerkin Isogeometric Analysis that is explicit in h and p. *Comput. Methods Appl. Math.*, 2021. Online first.

[27] R. Schneckenleitner and S. Takacs. Towards a IETI-DP solver on non-matching multi-patch domains. In *Domain Decomposition Methods in Science and Engineering XXVI*, 2021. To appear. `https://arxiv.org/pdf/2103.02536.pdf`.

[28] S. Takacs. Discretization error estimates for discontinuous Galerkin Isogeometric Analysis. *Appl. Anal.*, 2021. To appear. `https://arxiv.org/abs/1901.03263`.

Latest Reports in this series

2009 - 2019

[..]

2020

2020-01	Ioannis Toulopoulos *Viscoplastic Models and Finite Element Schemes for the Hot Rolling Metal Process*	February 2020
2020-02	Rainer Schneckenleitner and Stefan Takacs *Convergence Theory for IETI-DP Solvers for Discontinuous Galerkin Isogeometric Analysis That Is Explicit in h and p*	May 2020
2020-03	Svetoslav Nakov and Ioannis Toulopoulos *Convergence Estimates of Finite Elements for a Class of Quasilinear Elliptic Problems*	May 2020
2020-04	Helmut Gfrerer, Jiří V. Outrata and Jan Valdman *On the Application of the Semismooth* Newton Method to Variational Inequalities of the Second Kind*	July 2020

2021

2020-01	Ioannis Toulopoulos *A Continuous Space-Time Finite Element Scheme for Quasilinear Parabolic Problems*	February 2021
2020-02	Rainer Schneckenleitner and Stefan Takacs *Towards a IETI-DP Solver on Non-Matching Multi-Patch Domains*	March 2021
2020-03	Rainer Schneckenleitner and Stefan Takacs *IETI-DP for Conforming Multi-Patch Isogeometric Analysis in Three Dimensions*	March 2021
2020-04	Ulrich Langer *Adaptive Space-Time Finite Element and Isogeometric Analysis*	March 2021
2021-05	Helmut Gfrerer and Jiří V. Outrata *On Subspaces Contained in Generalized Derivatives and Strong Metric (Sub)regularity*	June 2021
2021-06	Ioannis Toulopoulos *A Unified Stable Space-Time Finite Element Scheme for Non-Newtonian Power Law Models*	August 2021
2021-07	Rainer Schneckenleitner and Stefan Takacs *IETI-DP Methods for Discontinuous Galerkin Multi-Patch Isogeometric Analysis with T-junctions*	September 2021

From 1998 to 2008 reports were published by SFB013. Please see
`http://www.sfb013.uni-linz.ac.at/index.php?id=reports`
From 2004 on reports were also published by RICAM. Please see
`http://www.ricam.oeaw.ac.at/publications/`
For a complete list of NuMa reports see
`http://www.numa.uni-linz.ac.at/Publications/List/`